

# NOTE: Titan's Atmosphere in Late Southern Spring Observed with Adaptive Optics on the W. M. Keck II 10-meter Telescope<sup>1</sup>

Henry G. Roe,<sup>2</sup> Imke de Pater,<sup>2</sup> Bruce A. Macintosh,<sup>3</sup> Seran G. Gibbard,<sup>3</sup> Claire E. Max,<sup>3</sup>  
and  
Chris P. McKay<sup>4</sup>

*Icarus*, in press.

## ABSTRACT

Using adaptive optics on the W.M. Keck II telescope we imaged Titan several times during 1999 to 2001 in narrowband near-infrared filters selected to probe Titan's stratosphere and upper troposphere. We observed a bright feature around the south pole, possibly a collar of haze or clouds. Further, we find that solar phase angle explains most of the observed east-west brightness asymmetry of Titan's atmosphere, although the data do not preclude the presence of a 'morning fog' effect at small solar phase angle.

*Subject headings:* Titan; Satellites, Atmospheres; Infrared Observations

## 1. Introduction

Previous high-angular resolution studies of Titan have focused for the most part on mapping surface albedo (Meier *et al.* 2000; Gibbard *et al.* 1999; Combes *et al.* 1997; Smith *et al.* 1996; Coustenis *et al.* 2001). Several of these works derived atmospheric parameters, such as haze opacity, in order to separate the atmospheric and surface contributions. Most recently, Coustenis *et al.* (2001) used moderate bandwidth filters ( $\sim 0.15\mu\text{m}$  FWHM) in the J- and H-bands on the 3.6 m Canada-France-Hawaii Telescope to image the surface and detected increased limb brightening around Titan's South Pole and on Titan's morning limb. Titan's morning limb is to the East on the sky as viewed from Earth. Coustenis *et al.* (2001)'s observations were just past Titan opposition from Earth with a Sun-Titan-Earth angle of only  $0^\circ.5$ . If, as one might expect, solar phase angle determines the East-West asymmetry in limb-brightening, then Coustenis *et al.* (2001) would have seen increased limb brightening on Titan's evening limb. They interpreted this discrepancy from expectation by suggesting that a 'morning

fog' exists on Titan due to small diurnal changes in the thermal structure of the atmosphere and condensation of ethane as a parcel of air moves from the dark side of Titan to the sunlit side. The data we present here show that at larger solar phase angles, solar phase angle dominates the East-West limb-brightening asymmetry; however, our results are consistent with a 'morning fog' which would determine the East-West limb-brightening asymmetry at smaller phase angles. We also resolve the brightening seen at the southern limb by Coustenis *et al.* (2001) and Meier *et al.* (2000) into a 'collar' around the south pole at a planetographic latitude of  $70^\circ\text{S}$  to  $75^\circ\text{S}$ .

Since October 1999 we have imaged Titan using the adaptive optics (AO) system on the W.M. Keck II telescope (Wizinowich *et al.* 2000) in several narrowband filters. In this Note we present the data from narrowband filters centered at  $1.158\mu\text{m}$  and  $1.702\mu\text{m}$ , chosen to probe only the upper atmosphere of Titan above the middle-to-upper troposphere ( $>\sim 20\text{ km}$  altitude). The contribution from surface reflection is negligible; essentially all the light we observe in these filters is sunlight scattered by particles in the atmospheric haze layers (Lemmon *et al.* 1995). These images show a number of features in Titan's atmosphere: a bright collar around Titan's south pole, northern polar limb-brightening, and an east-west asymmetry in limb-brightening.

## 2. Observations

The images presented in this Note were obtained on the dates listed in Table 1. The October 1999 data were taken 7.1 days before opposition, with a Sun-Titan-Earth angle of  $\sim 0^\circ.9$ . The Au-

<sup>1</sup>Data presented herein were obtained at the W.M. Keck Observatory, which is operated as a scientific partnership among the California Institute of Technology, the University of California, and the National Aeronautics and Space Administration. The Observatory was made possible by the generous financial support of the W.M. Keck Foundation.

<sup>2</sup>Department of Astronomy, 601 Campbell Hall, University of California, Berkeley, CA 94720-3411. Email address of the corresponding author: hroe@astro.berkeley.edu

<sup>3</sup>Lawrence Livermore National Laboratory, Livermore, CA 94550

<sup>4</sup>NASA Ames Research Center, Moffett Field, CA 94035

TABLE 1  
PARAMETERS OF TITAN OBSERVATIONS.

UT Date	UT Time	Filter	Exposure Time	Apparent Size <sup>a</sup>	Sub-Earth Latitude, Longitude <sup>a,b</sup>	Solar Phase Angle, Position Angle <sup>a,c</sup>
30 October 1999	11:00	J1158	3×120 sec	0''865	-19° 92, 108° 88	0° 8870, 91° 42
30 October 1999	11:36	H1702	3×120 sec	0''865	-19° 92, 109° 45	0° 8842, 91° 48
17 August 2000	15:36	J1158	4×120 sec	0''774	-24° 05, 208° 84	6° 3375, 77° 86
17 August 2000	15:13	H1702	4×120 sec	0''774	-24° 05, 208° 48	6° 3374, 77° 85
20 February 2001	6:24	J1158	4×120 sec	0''774	-23° 14, 108° 14	6° 1893, 256° 35
20 February 2001	5:50	H1702	4×120 sec	0''774	-23° 14, 107° 60	6° 1895, 256° 35

<sup>a</sup>Obtained from the JPL Horizons Ephemeris, available at <http://ssd.jpl.nasa.gov/horizons.html>

<sup>b</sup>Latitude and longitude coordinates are planetographic.

<sup>c</sup>These coordinates describe the position of the sub-Solar point relative to the sub-Earth point on Titan. The phase angle is defined as the Sun-Titan-Earth angle. The position angle (PA) is defined CCW with respect to direction of the true-of-date Celestial North Pole.

gust 2000 and February 2001 data are from opposite sides of opposition and the solar phase angle is nearly equal in size ( $\sim 6^\circ$ ) for these two data sets. Further details of the observations are listed in Table 1.

The data were collected using two different instruments. The October 1999 data were collected with KCAM, the Keck Observatory’s initial camera for use with Adaptive Optics (AO). KCAM contains a  $256 \times 256$  NICMOS-3 array with a platescale of  $0.0175''/\text{pixel}$ . Later data were collected using the slit-viewing camera SCAM of the observatory’s near-infrared spectrometer NIRSPEC (McLean *et al.* 1998). SCAM is a  $256 \times 256$  Rockwell HgCdTe array. When NIRSPEC is used behind the AO system a set of warm reimaging optics are used to form a platescale of  $0.017''/\text{pixel}$  on SCAM. In spite of the warm reimaging optics in front of SCAM, data from SCAM are of higher quality than data from KCAM due to a higher quality array, better optics, lower noise in the electronics, and a better baffled optical design with a true cold pupil stop. Between the AO bench and either instrument sits a room-temperature filter wheel, in which the narrowband filters used in the current work reside.

The filters used in the current work are IR bandpass filters purchased from Coherent<sup>5</sup>. The H1702 filter has a maximum transmission of 0.48 at a central wavelength of  $1.702 \mu\text{m}$  with a full-width-half-max (FWHM) of  $0.017 \mu\text{m}$ , and the J1158 filter has a maximum transmission of 0.58 at  $1.1582 \mu\text{m}$  with a FWHM of  $0.0175 \mu\text{m}$ . The appropriate internal cryogenic J- or H-band filter of NIRSPEC or KCAM is used to block any short or long wavelength light leaks of the J1158 and

H1702 filters.

Total exposure times for each image of Titan shown in Fig. 1 are listed in Table 1. Each night’s observations included a minimum of 3 images of Titan in different positions on the array to minimize the effect of bad pixels and noise in the flat-field correction. The sky background in both filters was observed to be extremely low ( $\ll 1 \text{ ct pixel}^{-1} \text{ sec}^{-1}$ ), in spite of each filter’s overlap of several night-sky OH lines (Rousselot *et al.* 2000). In some cases a separate sky frame at the same exposure length was obtained by offsetting 10-20'' from Titan. In cases without a separate sky frame, dark frames from the beginning or end of the night were used to construct a median dark, which was subtracted from the images of Titan. Correction for the variations in the flat-field or pixel-to-pixel sensitivity were made using data taken on the twilight sky in the broadband H filter without the H1702 filter, and in the broadband J filter without the J1158 filter. On several evenings we also took these flat-field frames with the H1702 filter. These flat-field data taken with the H1702 filter show a decrease in the signal-to-noise ratio from the wideband H flat-field data but no other significant differences. Similarly we found no significant difference between flat fields observed in the J-band with or without the J1158 filter.

After sky or dark subtraction and flat-field correction, the permanently bad pixels in each image are replaced with the median of the nearest 4 to 8 good pixels. Each image of Titan is then cross-correlated to every other image of Titan from the same evening in the same filter. Our cross-correlation algorithm sparsely samples the (x-y)-lag plane and homes in on the peak of the cross-correlation function with a near-minimum of computing time. A second step of the algorithm is to

<sup>5</sup><http://www.coherentinc.com/>

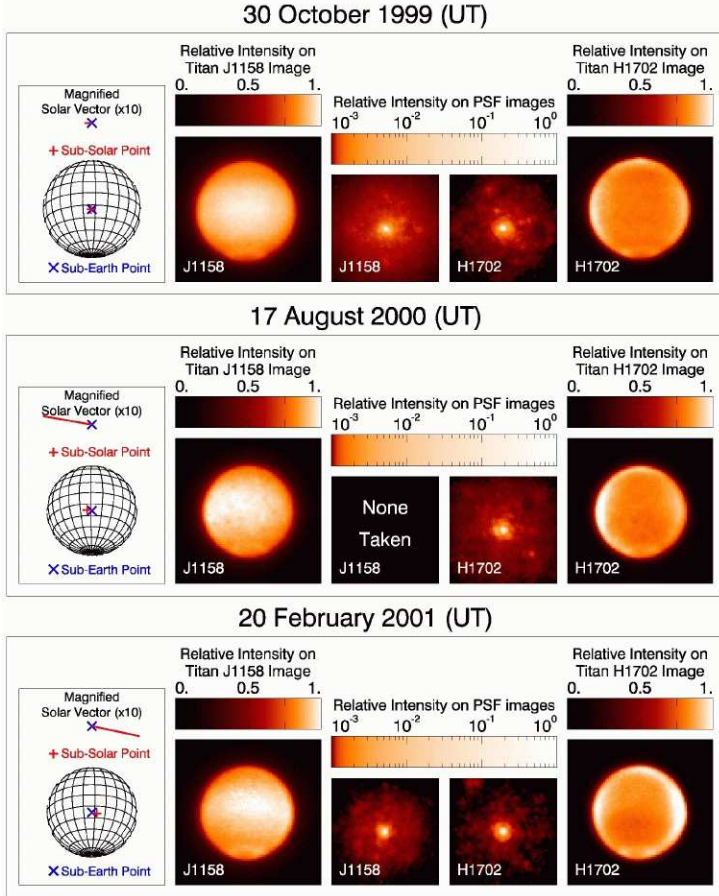


Fig. 1.— Images of Titan and PSF star. Each horizontal panel shows the observations from a different date. At left-most in each panel is a line figure showing the orientation of Titan’s disk and location of the sub-solar and sub-Earth points on Titan in the images for that date. Titan’s solid radius is 2575 km. The line figure of Titan’s orientation is shown at the same scale as Titan, assuming an apparent radius of 2650 km to partially account for the extent of Titan’s atmosphere, with lines of latitude and longitude plotted every  $15^\circ$ . Above this line figure is a graphic showing the direction and size of the vector from the sub-Earth point to the sub-solar point magnified by a factor of 10. The Titan J1158 images are all shown on the same linear color scale, as indicated by the color bars above the images. The Titan J1158 images were normalized such that the average intensity within the central  $\pm 4$  pixels is the same in all three images. Similarly, the Titan H1702 images are all shown on the same color scale, and were normalized such that the average intensity within the central  $\pm 6$  pixels is the same in all three images. The PSF images are all shown on logarithmic color scales relative to the peak intensity in each image.

then rebin each image by a factor of 4 (16 new pixels per 1 original pixel) and find the peak of the cross-correlation function to  $1/4$  pixel precision. We then do a linear-least squares fit to this matrix of offsets to find the shifts between all the images. The bad pixels in each image are remasked with zeroes before the final step of using bilinear interpolation to shift the images. Each pixel in the final coadded image is divided by the total exposure time it represents, which varies due to the masking of bad pixels. The final step of image processing was to rotate each image by the instrument position angle and Titan’s N-S position angle on the sky, such that Titan’s N-S axis aligns with the y-axis of the images shown in Figure 1. In the case of KCAM images, a flip about the vertical axis is necessary before this rotation in order to correct to the astronomical standard of sky north-up and sky east-left. Thus, the images of Titan in Fig. 1 are presented as Titan would normally be seen on the sky with Titan’s north-south axis aligned vertically.

In almost all cases a star of approximately the same visual magnitude as Titan was also observed before or after Titan in order to monitor the point spread function (PSF) of the AO correction. Processing of the PSF data is identical to the processing of the Titan data as described above, including the final step of image rotation so that the PSF images in Fig. 1 are at the same orientation as the corresponding images of Titan. Images of the PSF stars are shown on a logarithmic color scale in order to better display the wings of the PSF. The total exposure time each PSF image contains ranges from 10 to 100 sec. All data presented here were taken on nights of average to better-than-average seeing ( $\leq \sim 0''.5$ ). Images of the PSF stars show that the FWHM of the AO-corrected PSF was 45 to 48 milliarcsec in J1158 and 47 to 53 milliarcsec in H1702, both well sampled by our pixels of roughly 17 milliarcsec. These are within a factor of two of the theoretical limit for a 10-meter telescope ( $1.02 \lambda/D = 24$  milliarcsec at  $1.158 \mu\text{m}$  and  $36$  milliarcsec at  $1.702 \mu\text{m}$ ). A PSF with a FWHM of 50 milliarcsec means that the spatial resolution of our data is approximately 300 km referenced to Titan’s surface.

### 3. Atmospheric Calculations

While an attempt to fit these images with a scattering/absorbing radiative transfer model of Titan’s atmosphere is beyond the scope of this short Note, estimating the altitudes probed by our narrowband filters is useful for initial interpretation. Figure 2 shows the average roundtrip methane opacity encountered by a photon as a

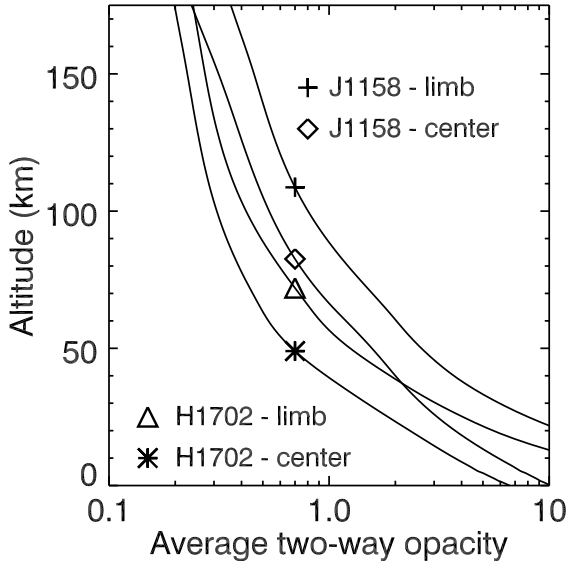


Fig. 2.— Altitudes probed by each filter. The y-axis is the altitude above Titan’s surface and the x-axis gives the average roundtrip methane opacity as a function of altitude as calculated using Eq. 2. Plotted are curves for both J1158 and H1702 filters at two different viewing points on Titan. The ‘center’ geometry is for a line of sight pointed straight at the center of Titan’s disk. The ‘limb’ geometry is for a line-of-sight at Titan’s limb that will cross just tangent to the solid surface. See text for more details on the definition of ‘average opacity’ in a filter. This figure shows that the H1702 filter probes several tens of kilometers deeper than the J1158 filter. Neither filter significantly probes the surface.

function of altitude. For each filter two cases are included. The first case is for a line-of-sight directed at the center of Titan’s disk. The second case is for a line-of-sight directed at Titan’s solid-surface limb. Our simple calculations ignore opacity due to haze scattering since at the wavelengths of our filters opacity due to methane is much greater than the opacity from all other sources. We use the profile of Yelle *et al.* (1997) for the atmospheric structure and methane abundance, and assume that each layer is a spherical shell. The methane abundance is 3% at the surface and in the troposphere, elsewhere the methane abundance is set to saturation. We use the self-broadened methane  $k$ -coefficients of Irwin *et al.* (1996) for these opacity calculations.

A more complete description of the correlated- $k$  method is given in Thomas and Stamnes (1999), but it is worth making explicit here what we mean by ‘average opacity’ for a filter. The Irwin *et al.* (1996)  $k$ -coefficients are calculated for 5  $\text{cm}^{-1}$  wide bins, and the bandwidths of both of our filters are covered by several tens of these wavenum-

ber bins. Our model atmosphere contains 326 layers which we number from  $l = 0$  at Titan’s surface to  $l = L_{top}$  at an altitude of 1300 km. Layers at altitudes  $> \sim 500$  km are essentially irrelevant for these current calculations. In wavenumber bin  $w$  the average roundtrip transmission from outside the atmosphere to the bottom of layer  $L$  and back out of the atmosphere is

$$T(w, L) = \sum_{i=0}^9 g_i \exp \left[ - \sum_{l=L}^{L_{top}} 2k_{i,l} u_l \right], \quad (1)$$

where:  $g_i$  is the weight of the  $i$ ’th Gaussian quadrature point of the  $k$ -distribution calculation, the abundance of methane  $u_l$  is calculated assuming that layer  $l$  is a spherical shell and that the atmosphere in layer  $l$  is homogeneous, and  $k_{i,l}$  is the Irwin *et al.* (1996)  $k$ -coefficient for the  $i$ ’th Gaussian quadrature point interpolated/extrapolated for the temperature and pressure of the  $l$ ’th atmospheric layer. The factor of 2 is included because we are interested in the roundtrip path. The ‘average’ opacity in a filter  $\tau(L)$  is then

$$\tau(L) = - \ln \left( \sum_{w=1}^W f_w T(w, L) \right) \quad (2)$$

where  $f_w$  is the relative transmissivity of the filter in each wavelength bin, normalized such that  $\sum_{w=1}^W f_w = 1.0$ . For the two filters J1158 and H1702 the average opacity of Eq. 2 is shown in Fig. 2.

#### 4. Observed Features: East-West Asymmetry

As discussed earlier, previous observers noted an asymmetry in the limb-brightening between the East/West or morning/evening limbs they could not attribute to phase angle effects. Coustenis *et al.* (2001) interpreted this as evidence for a ‘morning fog’ effect. Our images of Titan are displayed in the usual convention of Titan north up, with east-west displayed as they appear on the sky. Thus, given Titan’s prograde rotation, the morning limb is on the left in our images. If no winds exist the atmosphere at the morning limb is emerging from  $\sim 190$  hours of darkness. Given recent measurements of Titan’s zonal winds (Kostiuk *et al.* 2001), this period of darkness experienced by an atmospheric element could be as short as  $\sim 70$  hours. As described here, an initial interpretation of our data is consistent with, but does not require, a brightening of the morning limb beyond what would be expected due to phase angle considerations.

Our August 2000 and February 2001 images show obvious east-west asymmetry in both the

J1158 and H1702 filters. The asymmetry appears almost exactly reversed between these two dates of observation. As shown graphically in the left-most panels of Fig. 1, the solar phase angle is of almost exactly equal size ( $\sim 6^\circ$ ) and opposite direction on these two dates. In both cases the asymmetry is brighter in the direction of the sub-solar point, as would be expected if the asymmetry is to be explained by the solar phase angle.

The October 1999 data were taken at a much smaller solar phase angle ( $0.9^\circ$ ). In this case the J1158 image shows essentially no east-west asymmetry. On the other hand, the H1702 image exhibits an east-west asymmetry and the sign of the asymmetry is in agreement with the direction of the solar angle. Since these observations were taken before opposition this brightening is on the morning limb. Therefore, without more detailed analysis and modeling, these observations neither confirm nor rule out the presence of a ‘morning fog.’

We therefore conclude that our data show definitively that at larger solar phase angles the effect of the solar phase angle dominates the observed east-west asymmetry, but that our data do not rule out the ‘morning fog’ hypothesis of Coustenis *et al.* (2001) at small phase angles, but also do not appear to require such a hypothesis.

## 5. Observed Features: Southern Polar Collar and Northern Limb Brightening

All of the images presented here show a bright feature about the south pole and the H1702 images show a brightening at the Northern limb. This southern feature appears to be a bright collar with a hole centered on the south pole, rather than a cap covering the entire polar region. In the North-South direction the collar appears to be unresolved ( $< \sim 270$  km projected on our images, or  $< \sim 380$  km referenced to Titan’s surface at this latitude) and centered between  $70^\circ\text{S}$  and  $75^\circ\text{S}$  latitude. The J1158 images are typically limb-darkened, while the H1702 images are limb-brightened. A simplistic explanation for this difference can be understood by realizing that the light we are seeing is scattered off haze and that the bulk of this haze sits in the lower stratosphere where the opacity due to methane is significantly different at J1158 wavelengths versus H1702 wavelengths. At J1158 wavelengths the haze is embedded in greater methane opacity compared to H1702 wavelengths, leading to the observed difference in limb brightening and darkening.

From the transmission calculations presented in Fig. 2 it is clear that these features are atmospheric, rather than lying on Titan’s surface. Us-

ing the the average transmission curves of Fig. 2 we can draw some conclusions about the altitudes of these northern and southern features. The northern limb brightening is apparent in H1702 images, but is missing from J1158 images. The absence of this feature from the J1158 data indicates that this northern haze or cloud must lie below approximately 90 km altitude, where the ‘J1158-limb’ opacity is equal to unity. Similarly, the presence of the northern brightening in the H1702 data leads us to conclude that this northern haze or cloud sits more than 20-30 km above Titan’s surface. Titan’s tropopause is at approximately 40 km altitude. Therefore, our data constrain this northern atmospheric feature, at the time of the observations, to the lower stratosphere or upper troposphere.

Similar arguments can be made about the southern polar collar, which is apparent in both J1158 and H1702 images. No upper limit on the altitude of the haze or cloud forming this polar collar can be easily deduced without further radiative transfer modeling and data analysis. However, the presence of the collar in the J1158 data lead us to conclude that this collar of material must be at or above 40 to 50 km altitude. Thus, our data and calculations restrict the southern polar collar to be above the tropopause and at higher altitudes than the cloud or haze observed on the northern limb.

We suggest that these Northern and Southern features are of a seasonal origin. Voyager II in visible light saw a dark Northern polar collar or hood in early Northern Spring (Smith *et al.* 1982), while our observations are in late Southern Spring. It is possible that Voyager II’s Northern polar hood is of the same seasonal origin as the Southern Polar collar we observed. A plausible explanation, inspired by an investigation of  $\text{C}_4\text{N}_2$  by Samuelson *et al.* (1997), is that during the long dark winter of Titan’s poles significant gas-phase concentrations of reaction products such as  $\text{C}_4\text{N}_2$  accumulate. At or above super-saturated concentrations particles will condense out. Temperature in the polar stratosphere appears to lag behind insolation, such that during spring the polar stratosphere is actually cooling (Bezard *et al.* 1995). Thus, during spring as the polar stratosphere cools the rate of condensation of these particles is enhanced. Assuming some combination of: continued condensation of new particles into late spring as the polar atmosphere reaches its annual minimum temperature, with particle fall-out times of  $> \sim 1$  Earth year, we would expect to see the remains of this polar winter buildup through late spring. Such a phenomenon matches what we observe near Titan’s south pole. Further, a large buildup of haze

particles over the northern winter pole could be expected to extend to latitudes just south of the fully shadowed polar region, giving an explanation for the bright feature we see at Titan's northern limb.

In this hypothesis for explaining the southern polar collar we would expect the collar to fade in prominence and possibly disappear as spring progresses towards the southern summer equinox in late 2002. From October 1999 to February 2001 the southern feature does not appear to change significantly. To better understand the seasonal cycles on Titan we must continue to observe. We intend to continue monitoring Titan's atmosphere using this relatively new technique of adaptive optics on large telescopes through the arrival of the Cassini mission in 2004 and beyond.

### Acknowledgements

We thank the staff of the W.M. Keck Observatory, especially the members of the adaptive optics team for all their hard work. H.G.R. acknowledges support from a NASA GSRP grant funded through NASA Ames Research Center and a Sigma Xi Grant-in-Aid-of-Research from the National Academy of Sciences, through Sigma Xi, The Scientific Research Society. This work was performed under the auspices of the U.S. Department of Energy, National Nuclear Security Administration by the University of California, Lawrence Livermore National Laboratory under contract No. W-7405-Eng-48. This work has been supported in part by the National Science Foundation Science and Technology Center for Adaptive Optics, managed by the University of California at Santa Cruz under cooperative agreement No. AST-9876783. The authors wish to extend special thanks to those of Hawaiian ancestry on whose sacred mountain we are privileged to be guests. Without their generous hospitality, none of the observations presented herein would have been possible.

### REFERENCES

Bezard, B., A. Coustenis, C.P. McKay 1995. Titan's Stratospheric Temperature Asymmetry: A Radiative Origin? *Icarus* **113**, 267-276.  
 Combes, M., L. Vapillon, E. Gendron, A. Coustenis, O. Lai, R. Wittemberg, and R. Sirdey 1997. Spatially resolved images of Titan by means of adaptive optics. *Icarus* **129**, 482-497.  
 Coustenis, A. E. Gendron, O. Lai, J.-P. Véran, J. Woillez, M. Combes, L. Vapillon, T. Fusco, L. Mugnier, and P. Rannou 2001. Images of Titan at 1.3 and 1.6 micron with adaptive optics at the CFHT. *Icarus*, in press.  
 Gibbard, S.G. B. Macintosh, D. Gavel, C.E. Max, I. de Pater, A.M. Ghez, E.F. Young, and C.P.

McKay 1999. Titan: High-resolution speckle images from the Keck telescope. *Icarus* **139**, 189-201.  
 Griffith, C.A., T. Owen, G.A. Miller, and T. Geballe 1998. Transient clouds in Titan's lower atmosphere. *Nature* **395**, 575-578.  
 Irwin, P.G.J., S.B. Calcutt, F.W. Taylor, and A.L. Weir, 1996. Calculated K distribution coefficients for hydrogen- and self-broadened methane in the range 2000-9500  $\text{cm}^{-1}$  from exponential sum fitting to band-modelled spectra. *J. Geophys. Res.* **101**, 26137-26154.  
 Kostiuk, T., K.E. Fast, T.A. Livengood, T. Hewagama, J.J. Goldstein, F. Espenak, and D. Buhl, 2001. Direct Measurement of Winds on Titan. *Geophys. Res. Letters* **28**, 2361-2364.  
 Lemmon, M.T., E. Karkoschka, and M. Tomasko 1995. Titan's Rotational Light-Curve. *Icarus* **113**, 27-38.  
 McLean, I.S., and 14 colleagues, 1998. Design and development of NIRSPEC: a near-infrared echelle spectrograph for the Keck II telescope. *Proc. SPIE* **3354**, 566-578.  
 Meier, R., B.A. Smith, T.C. Owen, and R.J. Terile 2000. The Surface of Titan from NICMOS Observations with the Hubble Space Telescope. *Icarus* **145**, 462-473.  
 Rousselot, P., C. Lidman, J. Cuby, G. Moreels, and G. Monnet 2000. Night-sky spectral atlas of OH emission lines in the near-infrared. *Astron. Astrophys.* **354**, 1134-1150.  
 Samuelson, R.E., L.A. Mayo, M.A. Knuckles, and R.J. Khanna, 1997.  $\text{C}_4\text{N}_2$  ice in Titan's north polar stratosphere. *Planet. and Space Sci.* **45**, 941-948.  
 Smith, B.A., and 28 colleagues, 1982. A New Look at the Saturn System: The Voyager 2 Images. *Science* **215**, 504-537.  
 Smith, P.H., M.T. Lemmon, and R.D. Lorenz 1996. Titan's surface, revealed by HST imaging. *Icarus* **119**, 336-349.  
 Thomas, G. E. and K. Stamnes 1999. *Radiative Transfer in the Atmosphere and Ocean*. Cambridge Univ. Press, Cambridge.  
 Wizinowich, P., and 17 colleagues, 2000. First Light Adaptive Optics Images from the Keck II Telescope: A New Era of High Angular Resolution Imagery. *PASP* **112**, 315-319.  
 Yelle, R. V., D. Strobel, E. Lellouch, and D. Gautier, 1997. Engineering models for Titan's atmosphere. In *Huygens: Science, Payload and Mission* (J.-P. Lebreton, Ed.) *Eur. Space Agency ESA SP* 1177, 243-256.

---

This 2-column preprint was prepared with the AAS L<sup>A</sup>T<sub>E</sub>X macros v5.0.